

Electronic Supplementary Information (ESI)

**Full-type photoluminescence from a single organic molecule
for multi-signal temperature sensing**

Jing Ma,^{a†} Yusheng Zhou,^{a†} Haiyang Gao,^a Fangming Zhu^b and Guodong Liang^{*a}

^aPCFM Lab, School of Materials Science and Engineering, Sun Yat-sen University,

Guangzhou 510275 (P.R. China). E-mail: lgdong@mail.sysu.edu.cn

[†]These authors contributed equally to this work

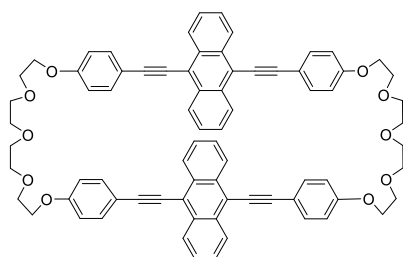
^bPCFM Lab, School of Chemistry, Sun Yat-sen University, Guangzhou 510275 (P.R.

China).

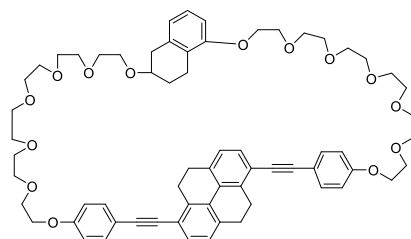
Table of Contents

1. Organic compounds reported with thermoresponsive photoluminescence (TRP)
2. Characterization
3. Materials and preparation
4. Microstructure, photophysical and thermal properties of TBBU
5. Thermal properties of TBBU
6. Single crystal data
7. Time-dependent density functional theory (TD-DFT) calculations and determination of constant
8. Temperature sensing using PLIA based on TBBU crystals
9. TBBU doped polymer films
10. Temperature sensing using PLIA based on TBBU doped polymer films
11. Testing the temperature of ice using PLIA based on the doped polymer films
12. Sensing temperature gradient using PLIA based on the doped polymer films

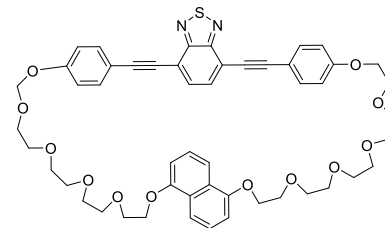
1. Organic compounds reported with thermoresponsive photoluminescence (TRP)



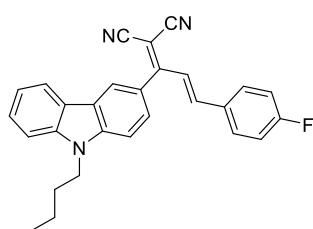
(annealing at 250 °C, emission color changes, crystal transition)¹



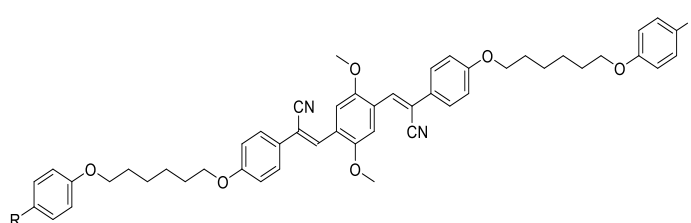
(annealing at 80 °C, emission color changes, crystallization)²



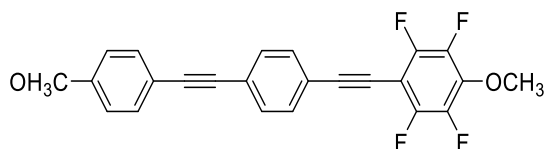
(annealing at 60 °C, emission color changes, crystallization)³



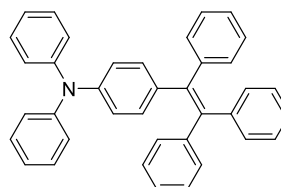
(heating at 150 °C, emission color changes, melting)⁴



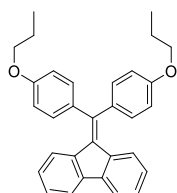
(grinding at 100 °C, emission color changes, crystal transition)⁵



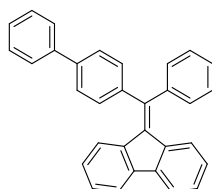
(heating at 200 °C, emission weakens, melting)⁶



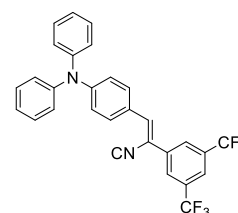
(heating at 120 °C, emission color changes, crystallization)⁷



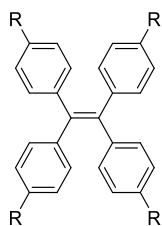
(heating at 120 °C, emission color changes, crystal transition; heating at 148 °C, emission weakens, melting)⁸



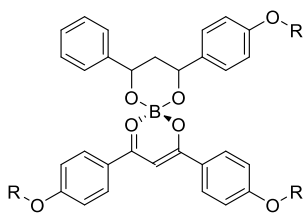
(annealing at 160 °C, emission is enhanced, crystallization)⁸



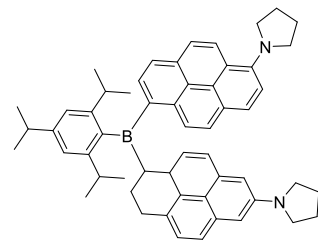
(heating at 135 °C, emission weakens, melting)⁹



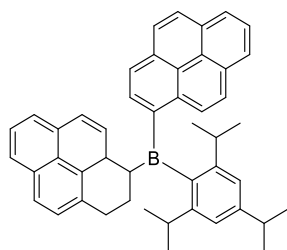
(-60 to 0 °C, emission color changes, glass transition; heating at 150 °C, emission weakens, melting)¹⁰



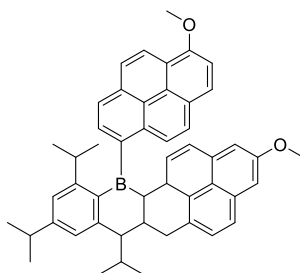
(-196 to 25 °C, emission color changes, twisted intramolecular charge transfer (TICT))¹¹



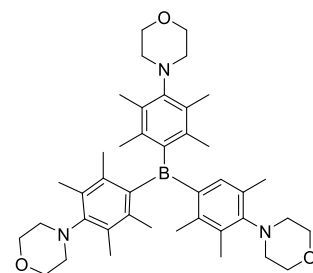
(-30 to 140 °C, emission color changes, TICT)¹²



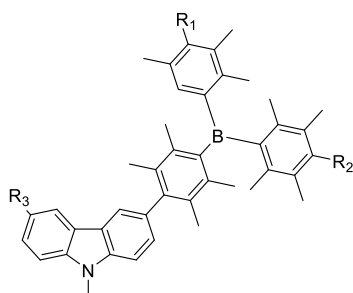
(-50 to 100 °C, emission color changes, TICT)¹³



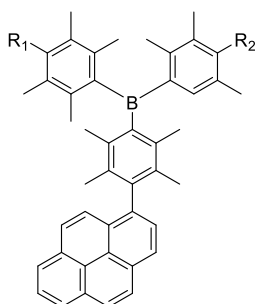
(-50 to 100 °C, emission color changes, TICT)¹⁴



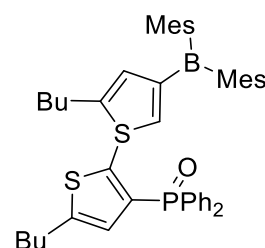
(-20 to 40 °C, emission color changes, TICT)¹⁵



(-196 to 20 °C, emission color changes, TICT)¹⁶



(0 to 150 °C, emission color changes, TICT)¹⁷



(-130 to 20 °C, emission color changes, charge transfer)¹⁸

Fig. S1 Chemical structures of organic compounds reported with thermoresponsive luminescence (TRL).

2. Characterization

UV-vis spectroscopy data were obtained using of a Lambda 950 instrument (Perkin Elmer).

Photoluminescence (PL) spectra, the lifetime and time-resolved emission spectra were recorded on an

Edinburgh Instruments LTD FLSP920 spectrofluorometer equipped with a vacuum chamber, a xenon arc lamp (Xe900), a microsecond flash-lamp (μ F900), a picosecond pulsed diode laser (EPL-345). Powder X-Ray diffraction (XRD) patterns were performed on a D-MAX 2200 VPC diffractometer (Rigaku) equipped with Ni-filtered Cu $K\alpha$ radiation, at a wavelength of 0.154 nm, at 40 kV and 26 mA. The samples were scanned in the 2θ range of 5–80 ° at a scan rate of 10 ° min⁻¹. The TGA curves were recorded using a Netzsch TG-209 thermobalance in a temperature arrangement of 30–450 °C at a heating rate of 10 °C min⁻¹ under nitrogen. Differential scanning calorimeter (DSC) analysis of TBBU crystals was carried out using a Perkin-Elmer DSC-7 Instrument under N₂ atmosphere. Single crystal data were collected on a Bruker CCD platform diffractometer. Data obtained with the ω - 2θ scan mode were collected on a Bruker SMART 1000 CCD diffractometer with graphite-monochromated Cu $K\alpha$ radiation (λ =1.54184 Å) or Mo $K\alpha$ radiation (λ =0.71073 Å). Photographs and videos of TBBU doped polymer films were recorded using a commercial iPhone SE. The morphology of TBBU was observed by scanning electron microscopy (SEM, Quanta 400, FEI Company). The fluorescence images of TBBU crystals and its doped polymer films were taken using a fluorescence microscope instrument (LEICA M205 FA).

3. Materials and preparation

3.1. Materials

N,N-Bis[4-(1,1-dimethylethyl)phenyl]-4-(4,4,5,5-tetramethyl-1,3,2-dioxaborolan-2-yl) benzeneamine (TBBU) has been synthesized in our laboratory previously.¹⁹ Other chemicals were all purchased from Energy Chemical in China and used as received without further purification unless otherwise indicated. Poly(ethylene oxide)/poly(propylene oxide) triblock copolymer (Pluronic F-127, E₁₂₆P₆₁E₁₂₆, E and P denoted repeat units of poly(ethylene oxide) and poly(propylene oxide) blocks, respectively, the subscripts

denoted the number of repeat units, $M_n=14600$ g/mol), polystyrene (PS), poly(methyl methacrylate) (PMMA) and fluororubber (FKM) were purchased from Aldrich (China) and used as received without further purification. THF and dichloromethane were purchased from *J&K* and distilled under normal pressure from sodium benzophenone ketyl under N_2 before use.

3.3 Preparation of TBBU doped polymer films

The preparation procedure of TBBU doped polymer films is described below. 45 mg of commercial polymer and 5 mg of TBBU were dissolved in 0.1 mL of DCM to get a clear solution. The resulted solution was cast on a clean glass wafer. The solvent was allowed to evaporate at room temperature overnight, yielding TBBU doped polymer films.

4. Microstructure, photophysical and thermal properties of TBBU

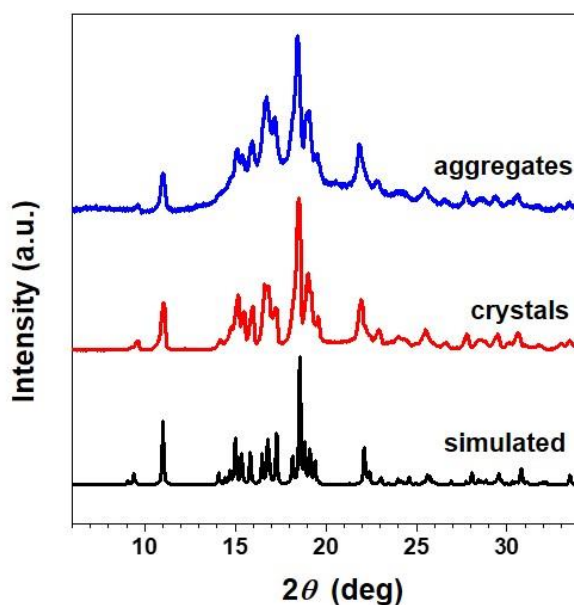


Fig. S2 XRD spectra of TBBU crystals and aggregates as well as the simulated spectrum from the single crystals.

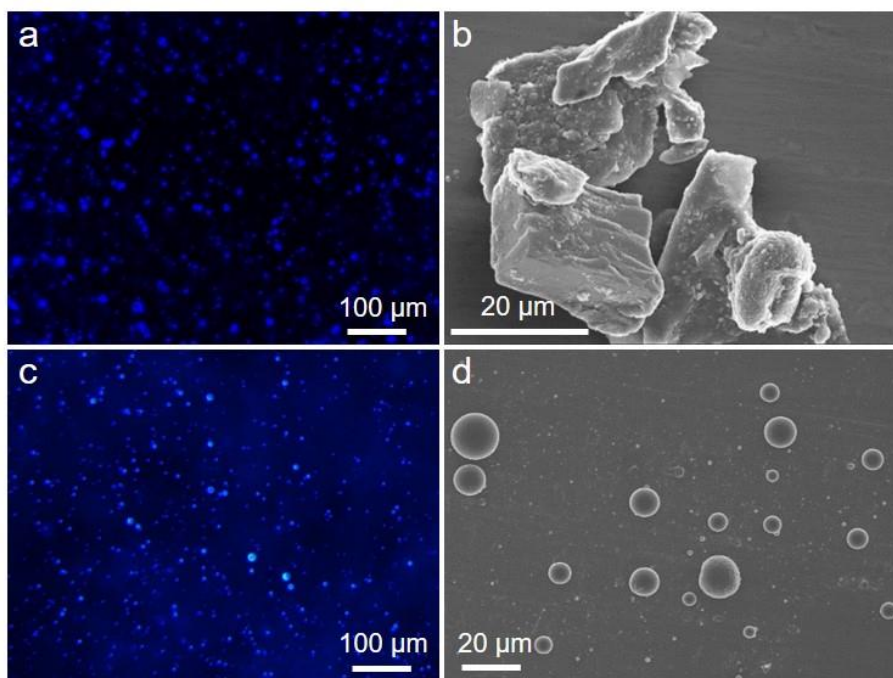


Fig. S3 Fluorescence microscopy (a, c) and scanning electron microscopy (b, d) images of the TBBU crystal films (a, b) and the aggregates in THF/H₂O mixture (containing 95% water) (c, d).

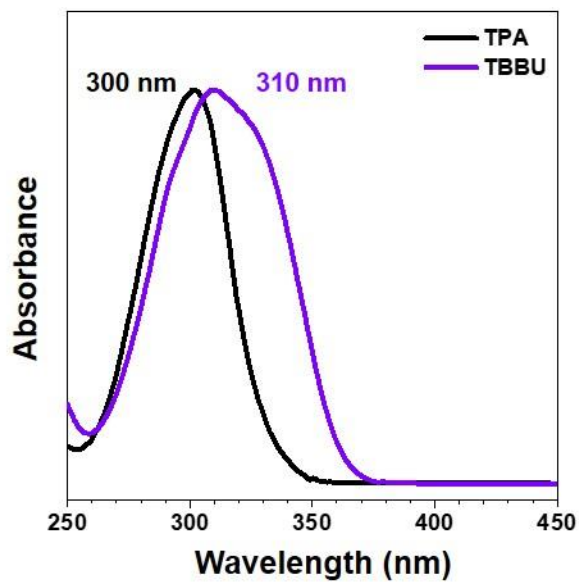


Fig. S4 UV-vis spectra of TBBU and triphenylamine (TPA) in DCM.

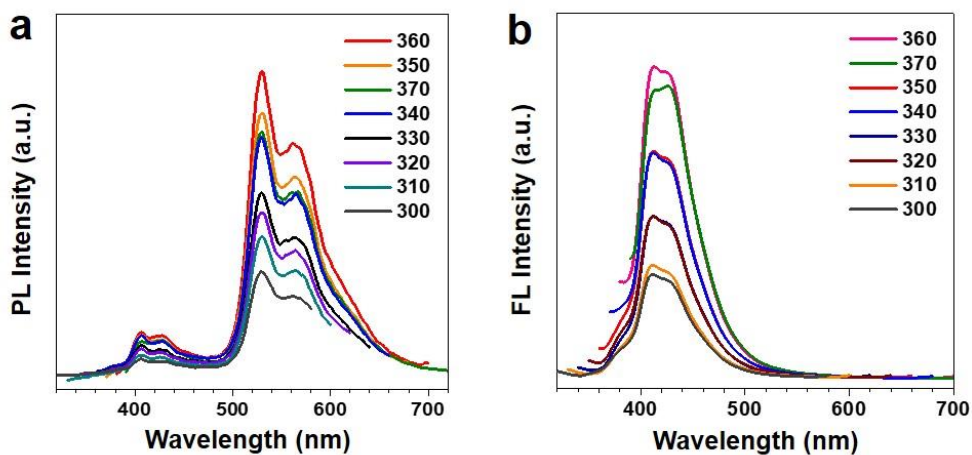


Fig. S5 Delayed PL spectra (by 8 ms) (a) and prompt PL spectra (b) of TBBU crystal films with different excitation wavelengths.

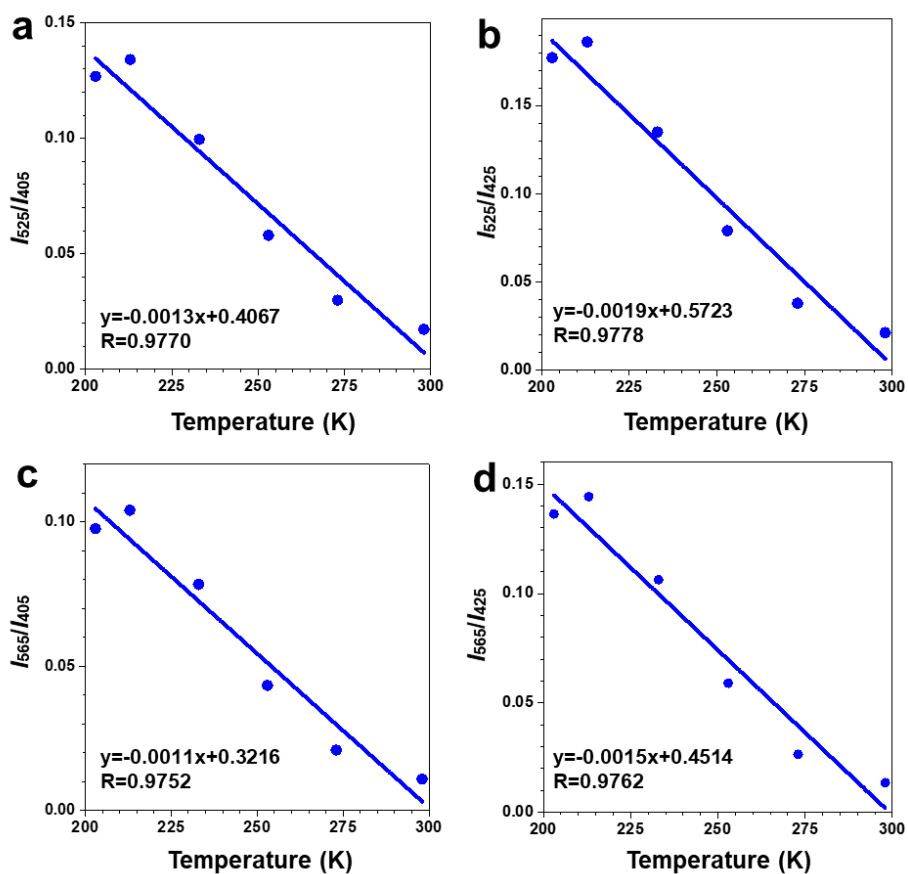


Fig. S6 Variation of phosphorescence intensity of the crystal films against temperature. I_{525} and I_{565} are the phosphorescence intensity at 525 and 565 nm, respectively. I_{405} and I_{425} are the fluorescence intensity at 405 and 425 nm, respectively.

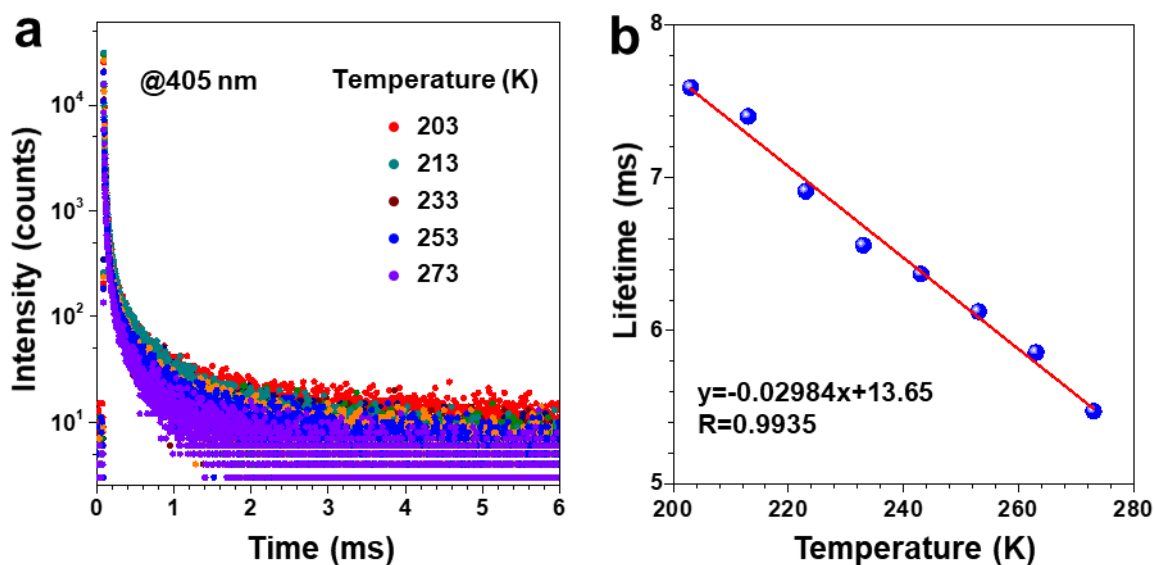


Fig. S7 (a) Lifetime decay profiles of the emission band (at 405 nm) at various temperatures (273, 253, 233, 213 and 203 K, from bottom to top, respectively) and (b) the plot of lifetime against temperature for the crystal films.

Table S1 Lifetime (at 405 nm) of TBBU crystal films at various temperatures.

Temperature (K)	Lifetime (ms)	τ_1 (ms)	P ₁ (%)	τ_2 (ms)	P ₂ (%)
203	7.589	0.7853	68.87	22.64	31.13
213	7.399	0.7988	68.81	21.96	31.19
223	6.911	0.7656	67.31	19.57	32.69
233	6.557	0.7407	66.61	18.16	33.39
243	6.370	0.7296	66.38	17.51	33.62
253	6.124	0.7676	65.28	16.20	34.72
263	5.857	0.6939	65.71	15.75	34.29
273	5.473	0.6704	65.58	14.62	34.42

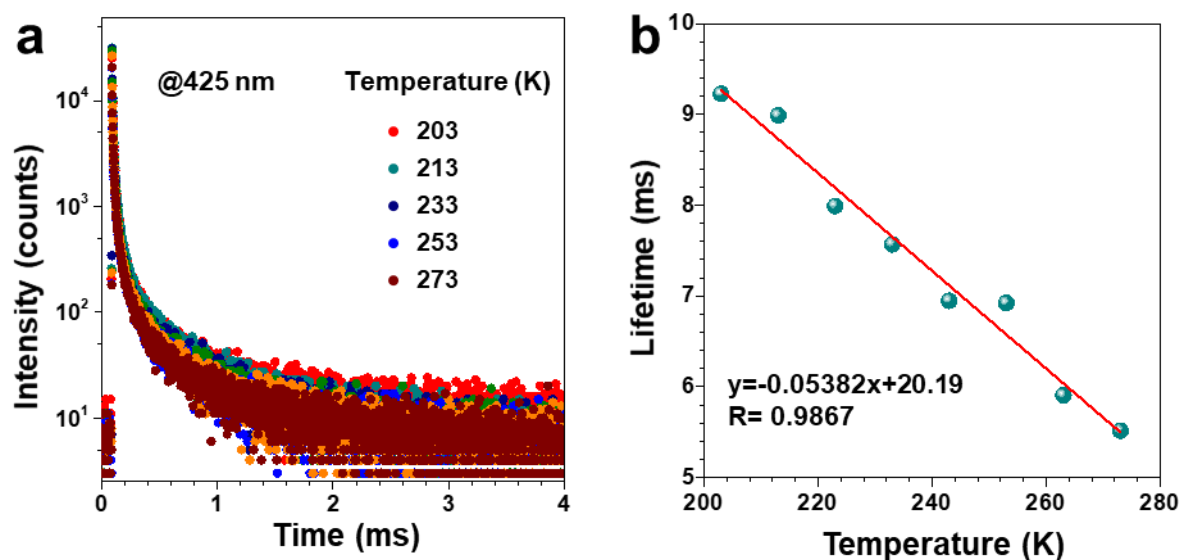


Fig. S8 (a) Lifetime decay profiles of the emission band (at 425 nm) at various temperatures (273, 253, 233, 213 and 203 K, from bottom to top, respectively) and (b) the plot of lifetime against temperature for the crystal films.

Table S2 Lifetime (at 425 nm) of TBBU crystal films at various temperatures.

Temperature (K)	Lifetime (ms)	τ_1 (ms)	P ₁ (%)	τ_2 (ms)	P ₂ (%)
203	9.227	0.9830	67.41	26.28	32.59
213	8.989	1.020	66.75	24.99	33.25
223	7.991	0.9011	65.4	21.39	34.6
233	7.569	0.9206	65.36	20.11	34.64
243	6.947	0.8333	64.36	17.99	35.64
253	6.924	0.8180	64.28	17.91	35.72
263	5.906	0.7059	64.64	15.41	35.36
273	5.516	0.6748	64.03	14.13	35.97

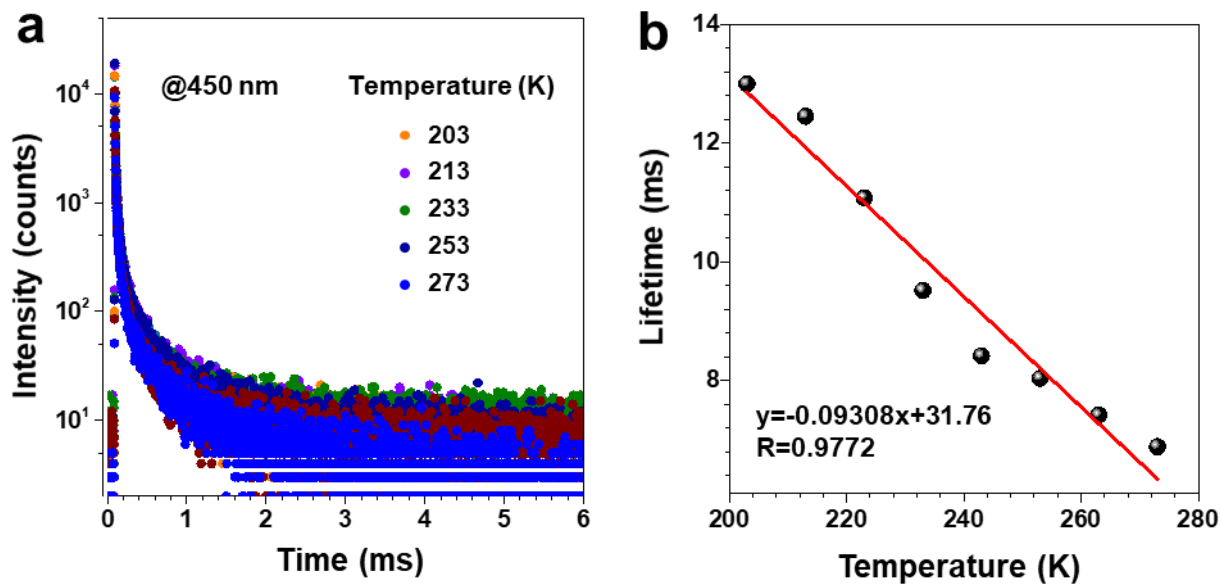


Fig. S9 (a) Lifetime decay profiles of the emission band (at 450 nm) at various temperatures (273, 253, 233, 213 and 203 K, from bottom to top, respectively) and (b) the plot of lifetime against temperature for the crystal films.

Table S3 Lifetime (at 450 nm) of the crystal films at various temperatures.

Temperature (K)	Lifetime (ms)	τ_1 (ms)	P ₁ (%)	τ_2 (ms)	P ₂ (%)
203	13.00	1.194	63.08	33.18	36.92
213	12.46	1.117	61.65	30.69	38.34
223	11.08	1.028	60.84	26.70	39.16
233	9.522	0.8889	60.74	22.88	39.26
243	8.421	0.8166	59.84	19.75	40.16
253	8.041	0.7881	58.92	18.46	41.03
263	7.423	0.8497	57.49	16.31	42.51
273	6.889	0.8407	58.52	15.42	41.48

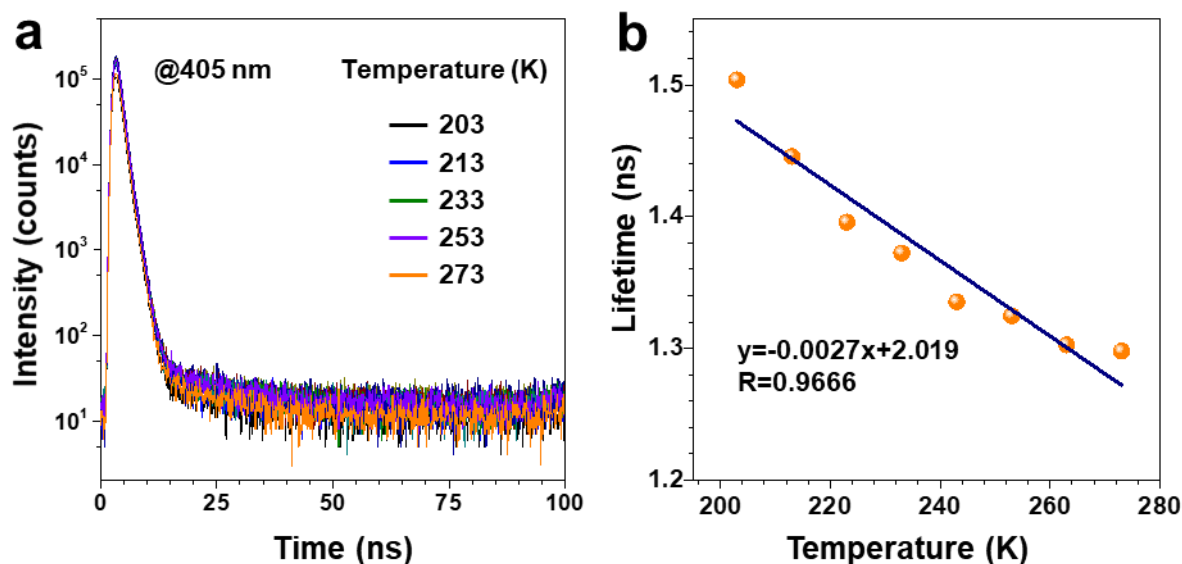


Fig. S10 (a) Lifetime decay profiles of the emission band (at 405 nm) at various temperatures (273, 253, 233, 213 and 203 K, from bottom to top, respectively) and (b) the plot of lifetime against temperature for the crystal films.

Table S4 Lifetime (at 405 nm) of the crystal films at various temperatures.

Temperature (K)	Lifetime (ns)	τ_1 (ns)	P ₁ (%)	τ_2 (ns)	P ₂ (%)
203	1.504	1.078	99.43	75.82	0.57
213	1.446	1.078	99.46	69.23	0.54
223	1.396	1.076	99.46	60.40	0.54
233	1.372	1.079	99.50	59.78	0.5
243	1.335	1.075	99.49	52.10	0.51
253	1.325	1.079	99.51	51.27	0.49
263	1.303	1.078	99.51	46.94	0.49
273	1.298	1.079	99.53	47.74	0.47

5. Thermal properties of TBBU

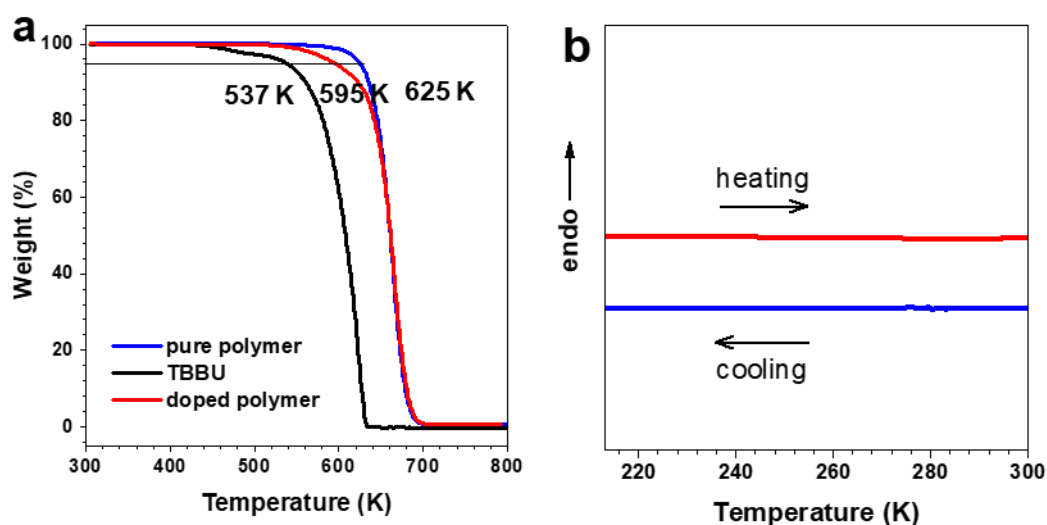


Fig. S11 (a) Thermogravimetry analysis (TGA) traces of TBBU crystals, pure polymer, and doped polymer and (b) differential scanning calorimetry (DSC) curves of TBBU crystals.

6. Single crystal data

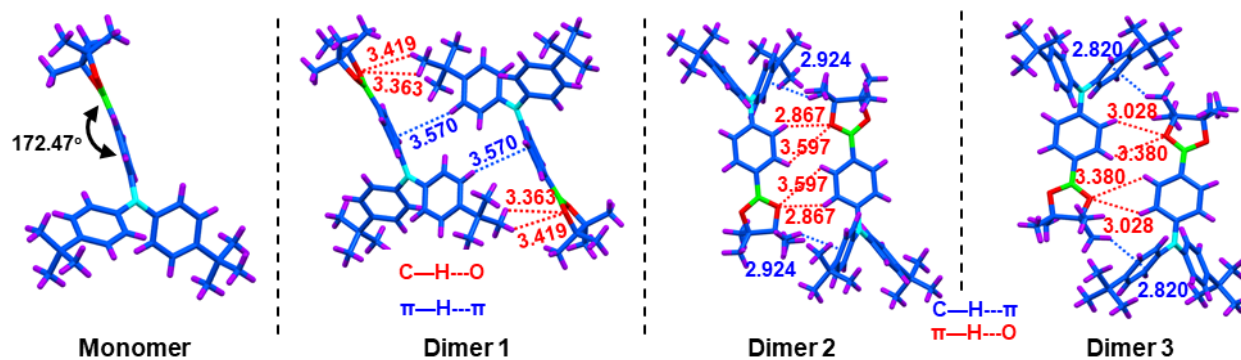


Fig.12 Intermolecular interaction between adjacent TBBU molecules in crystals.

7. Time-dependent density functional theory (TD-DFT) calculations and determination of constant

7.1 Computational methods

TD-DFT calculations were performed on Gaussian 09W program. Molecular geometry optimizations of

monomer and dimers were performed for the ground state (S_0) at the level of B3LYP using 6-31G(d) basis sets. The excitation energies including singlet state (S_n) and triplet state (T_n) were calculated at (TD-DFT) B3LYP/6-31G(d) level based on an optimized molecular structure at ground state (S_0).

Determination of nonradiative decay rate constant

$$\tau_p = 1/(k_p + k_{nr}) \quad \text{S1}$$

where k_p is the rate constant of phosphorescence, τ_p is the lifetime of phosphorescence, k_{nr} is the rate constant of nonradiative decay from T_1 to S_0 .

The phosphorescence lifetime of the chromophore crystals remained unchanged around 77 K in vacuum, thus nonradiative decay of the chromophore in the T_1 state was neglectable at 77 K in vacuum ($k_{nr}(77 \text{ K, vac}) \approx 0$), Therefore, k_p was calculated using $k_p = 1/\tau_p(77 \text{ K, vac})$ based on Equation S1. $k_{nr}(T)$ at each temperature was calculated using $k_{nr}(T) = 1/\tau_p(T) - k_p$.

Thus, k_p for the crystals is determined to be $k_p = 1/\tau_p(77 \text{ K, vac}) = 1/0.5957 = 1.679 \text{ s}^{-1}$.

k_p for the doped polymer films is determined to be $k_p = 1/\tau_p(77 \text{ K, vac}) = 1/0.5342 = 1.872 \text{ s}^{-1}$.

Table S5 The phosphorescence lifetime (τ_p) of the chromophore crystals and the doped polymer films at various temperatures in vacuum.

T (K)	the crystal (ms)	the polymer film (ms)
77	595.7	534.2
100	595.6	534.1
125	594.0	531.0
150	588.6	530.4
175	570.2	516.1
200	552.3	484.9

Table S6 The nonradiative decay rate constant from T₁ to S₀ (k_{nr}) for the crystal and doped films at various temperatures in air.

T (K)	the crystals (s ⁻¹)	the doped film (s ⁻¹)
203	0.697	1.035
213	0.939	1.489
223	1.298	2.157
233	1.878	3.090
243	2.713	5.175
253	4.078	7.605
263	5.622	12.413
273	7.249	23.184

Note: $k_p = 1.679 \text{ s}^{-1}$ for the crystals and $k_p = 1.872 \text{ s}^{-1}$ for the doped films.

Determination of quantum yield of phosphorescence

$$\Phi_p = \Phi_{isc} k_p \tau_p \quad \text{S2}$$

where Φ_p and Φ_{isc} are the quantum yield of phosphorescence from T₁ to S₀ and intersystem crossing (ISC) from S₁ to T₁, respectively. k_p is the rate constant of phosphorescence, τ_p is the lifetime of phosphorescence.

Table S7 Φ_p and Φ_{isc} for the crystals at various temperatures in air.

T (K)	Φ_p (%)	Φ_{isc} (%)
203	16.0	22.6
213	15.0	23.4
223	12.3	21.8
233	10.6	22.5
243	8.3	21.7
253	5.0	17.1
263	3.0	13.0
273	2.0	10.6

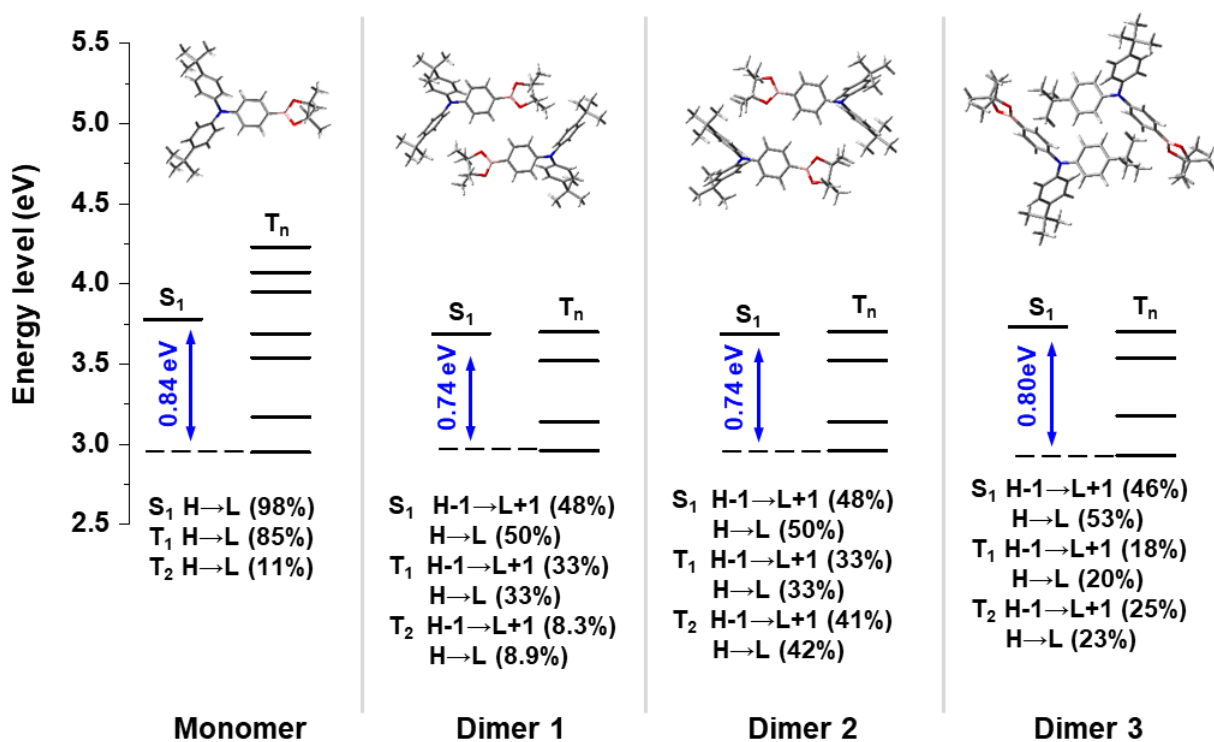


Fig. S13 The TD-DFT calculated singlet (S_1) and triplet (T_n) states for the monomer and corresponding dimers extracted from TBBU crystals at B3LYP/6-31G* level. The illustration shows the geometric arrangement of the dimers. Blue arrow and numbers indicate the energy difference (ΔE_{ST}) of the lowest singlet state (S_1) and the lowest triplet state (T_1)

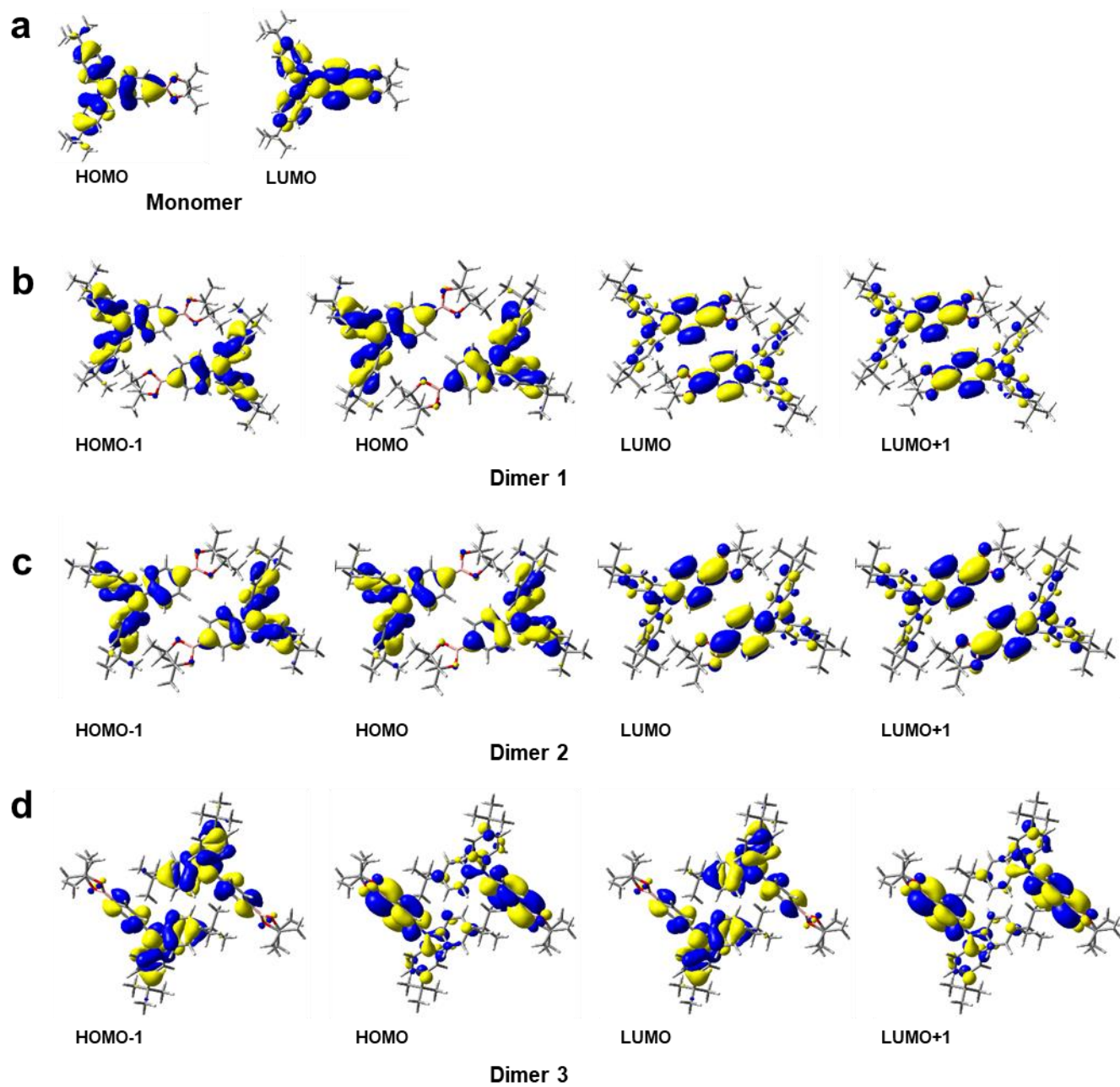


Fig. S14 (a) The involved frontier molecular orbitals for the (a) monomer and (b-d) corresponding dimers extracted from TBBU crystals.

8. Temperature sensing using PLIA based on TBBU crystal films

Table S8 The Lifetime and calculated temperature using PLIA based on TBBU crystals.

Designed temperature (K)	Fitting lifetime (ms)	Average lifetime (ms)	Calculated temperature (K)	Relative error (%)
203	423, 428, 430, 430, 429	428±2.9	202±0.66	1.92
213	381, 374, 383, 375, 387	380±5.4	212±1.1	1.80
223	334, 335, 324, 325, 336	331±5.8	223±1.3	0.925
233	282, 286, 282, 284, 287	284±2.3	232±0.16	1.39
243	234, 230, 230, 243, 244	236±6.9	243±1.5	1.06
253	185, 183, 182, 183, 183	183±1.1	254±0.47	4.48
263	148, 133, 121, 132, 140	134±10	265±2.1	12.9
273	94.4, 91.2, 72.3, 102, 102	92.4±12	273±2.6	0.165

9. TBBU doped polymer films

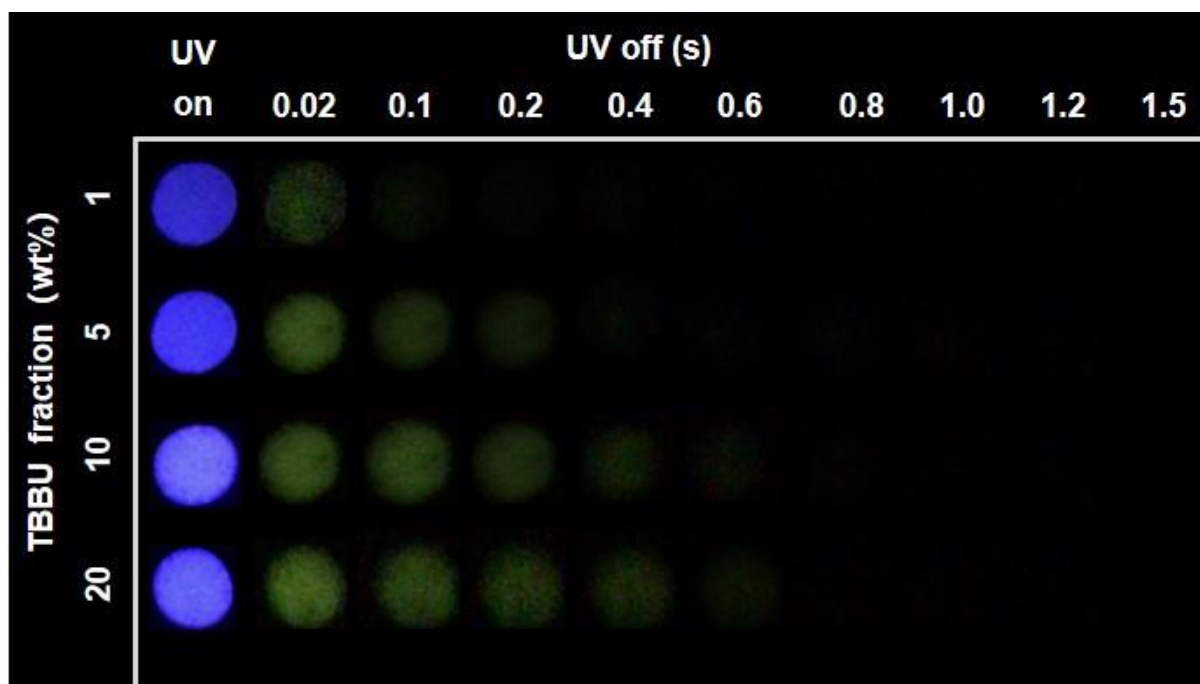


Fig. S15 Digital images of the TBBU doped polymer films at various doping fractions.

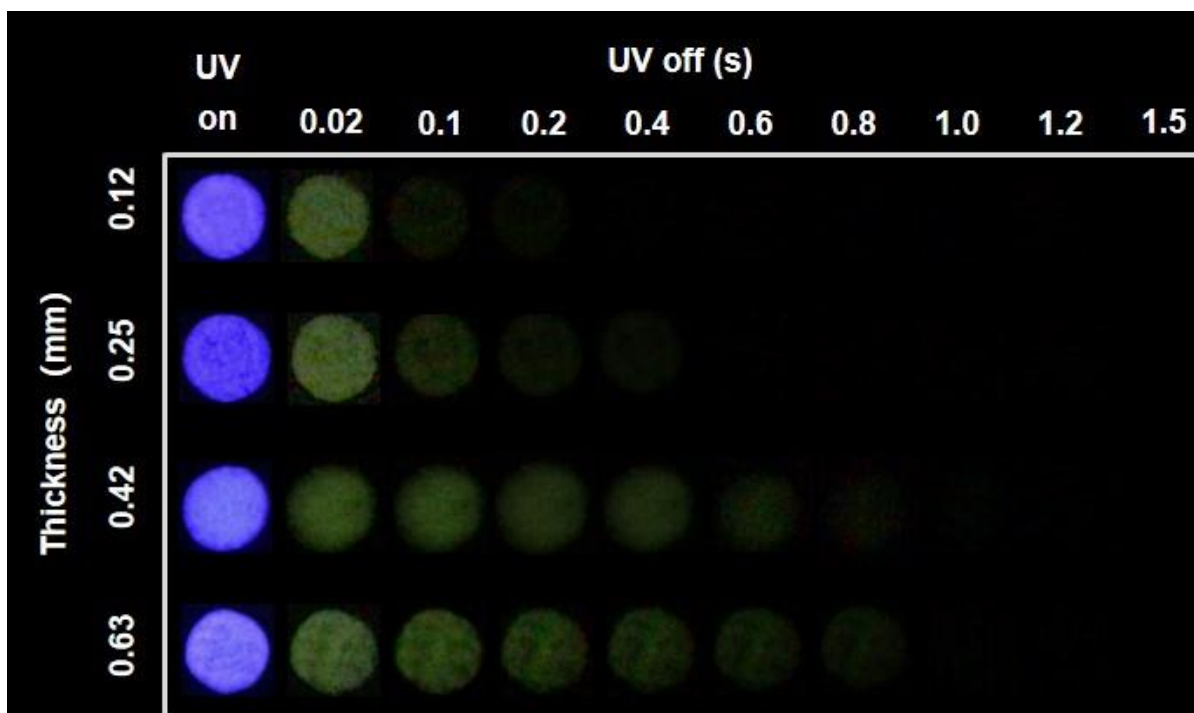


Fig. S16 Digital images of the TBBU doped polymer films with various thicknesses.

Table S9 Thickness of TBBU doped polymer films.

	1	2	3	4
Thickness (mm)	0.12, 0.12, 0.13, 0.11, 0.11	0.24, 0.24, 0.25, 0.26, 0.26	0.43, 0.42, 0.42, 0.41, 0.43	0.64, 0.62, 0.63, 0.62, 0.63
Average (mm)	0.12±0.008	0.25±0.01	0.42±0.008	0.63±0.008

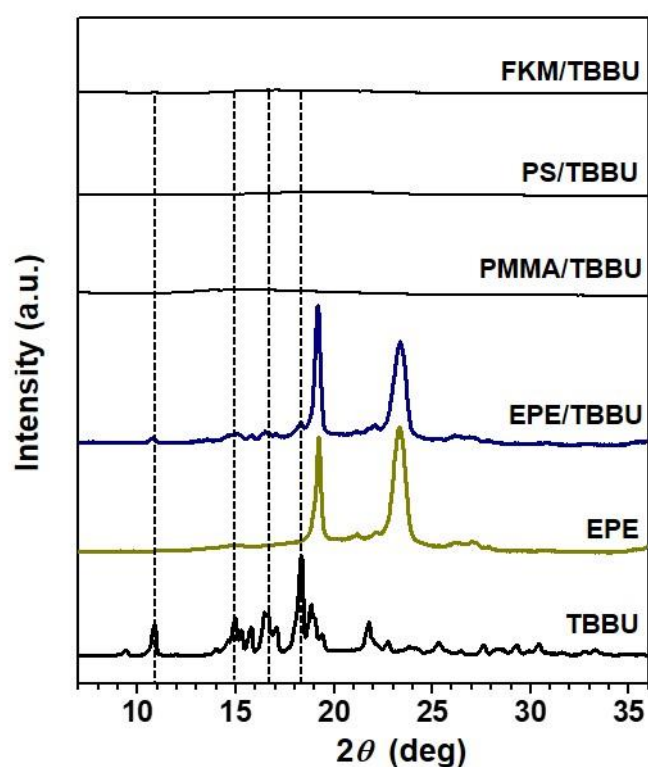


Fig. S17 XRD spectra of TBBU crystals and TBBU doped polymer films. EPE: poly(ethylene oxide)/poly(propylene oxide) triblock copolymer (Pluronic F-127), PMMA: poly(methyl methacrylate), PS: polystyrene, FKM: fluororubber.

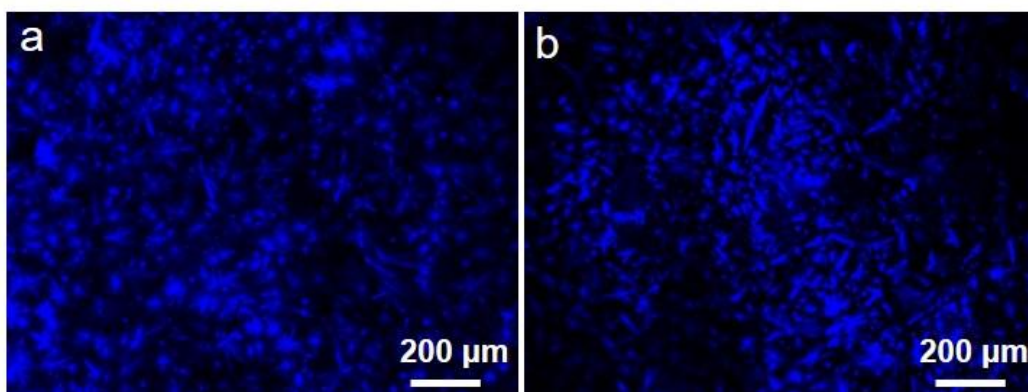


Fig. S18 Fluorescence microscopy images of the doped polymer films (a) and the etched films with methanol (b). The polymer was removed by methanol in (b).

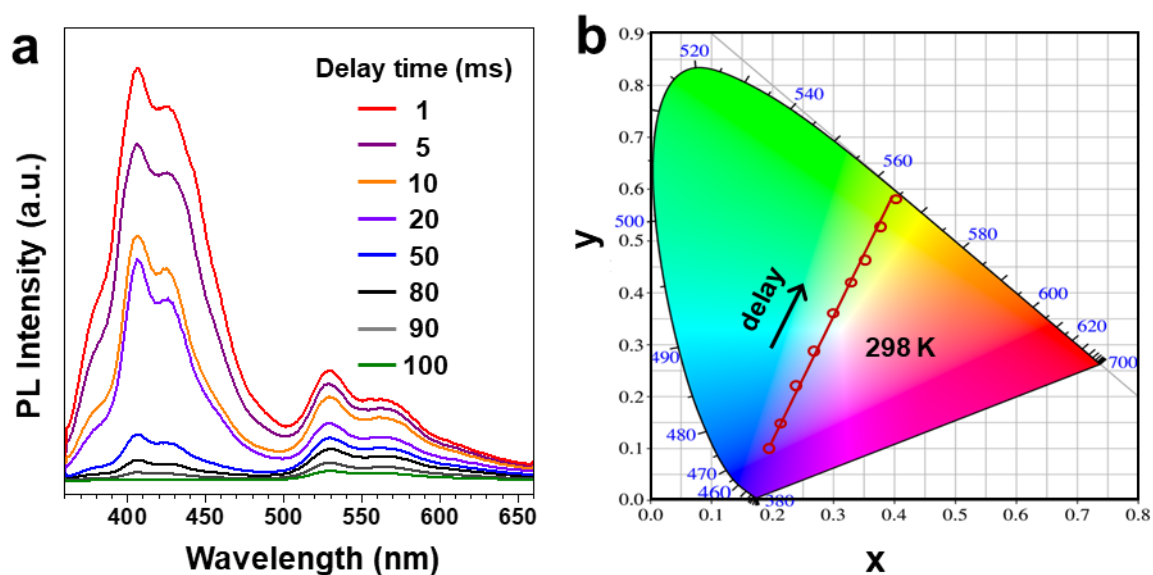


Fig. S19 (a) PL spectra delayed for various time of the polymer films (1, 5, 10, 20, 50, 80, 90 and 100 ms, from top to bottom, respectively). (b) The Commission Internationale de l'Eclairage (CIE) coordinates of the delayed PL spectra of the polymer films.

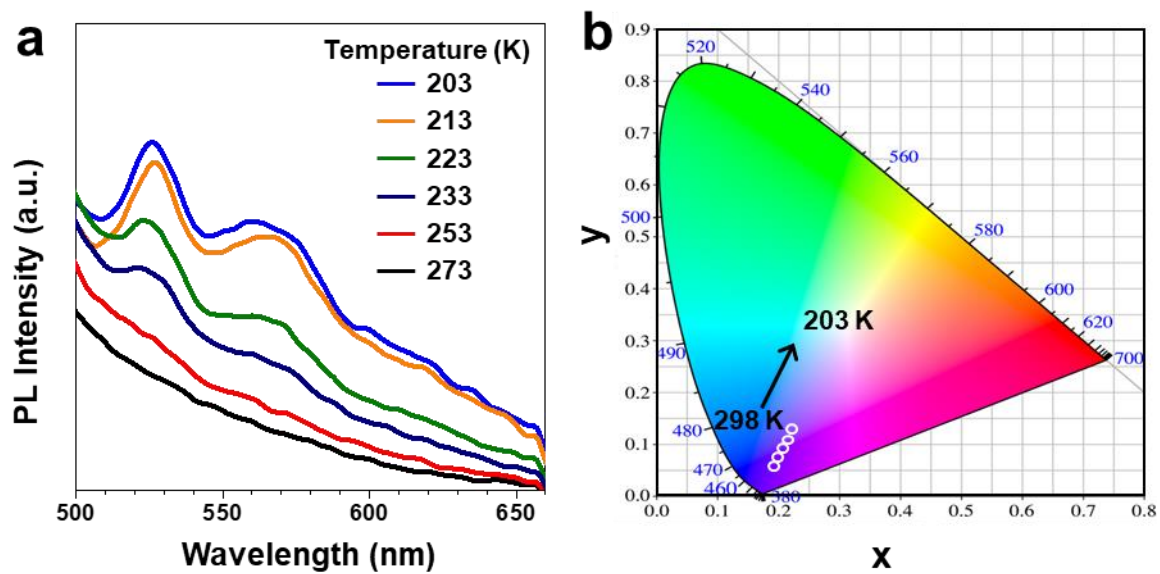


Fig. S20 (a) Prompt PL spectra of the doped polymer films at various temperatures (273, 253, 233, 223, 213 and 203 K, from bottom to top, respectively). (b) The Commission Internationale de l'Eclairage (CIE) coordinates of the PL spectra of the polymer films at various temperatures.

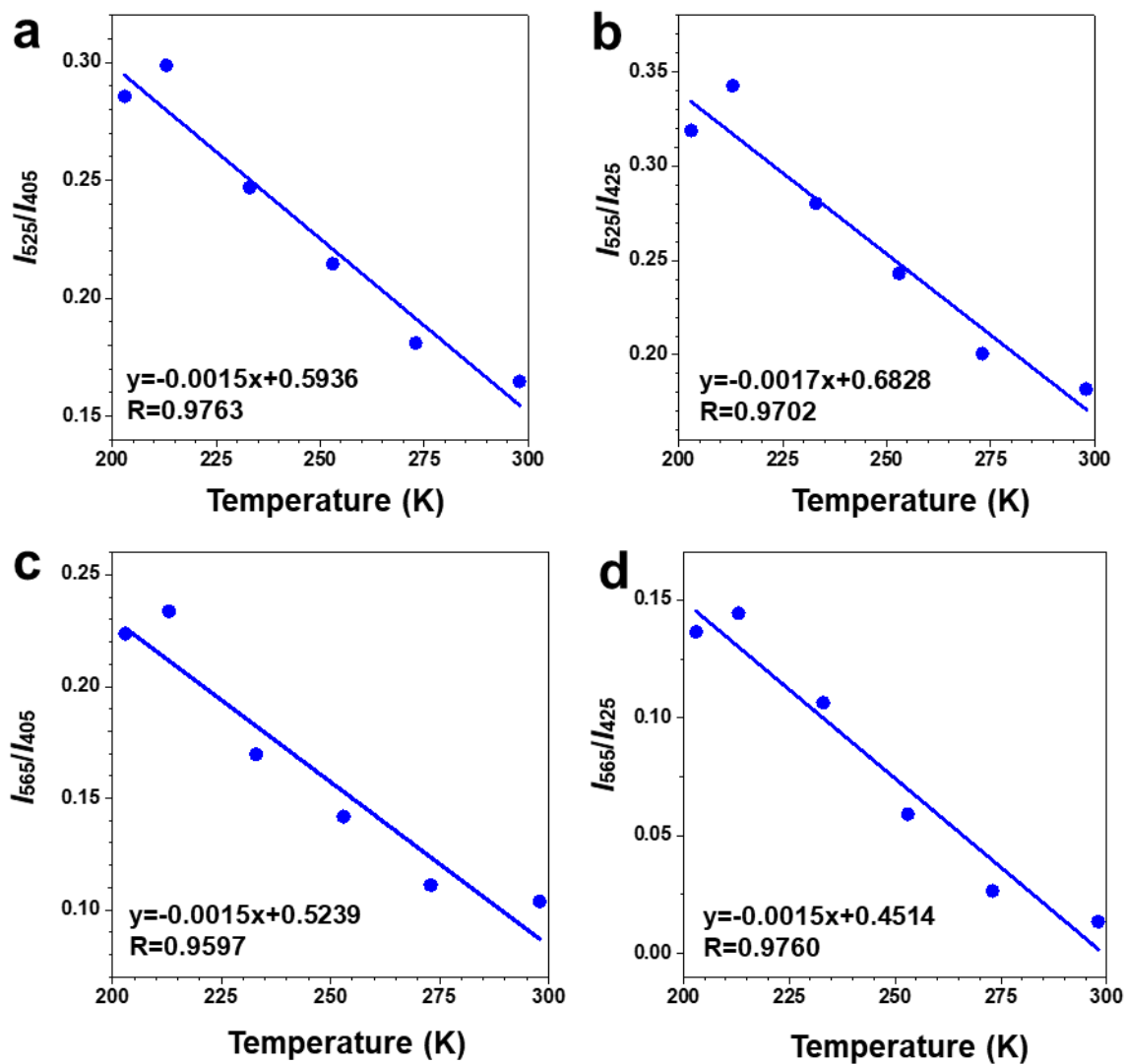


Fig. S21 Variation of phosphorescence intensity of the doped polymer films against temperature. I_{525} and I_{565} are the phosphorescence intensity at 525 and 565 nm, respectively. I_{405} and I_{425} are the fluorescence intensity at 405 and 425 nm, respectively.

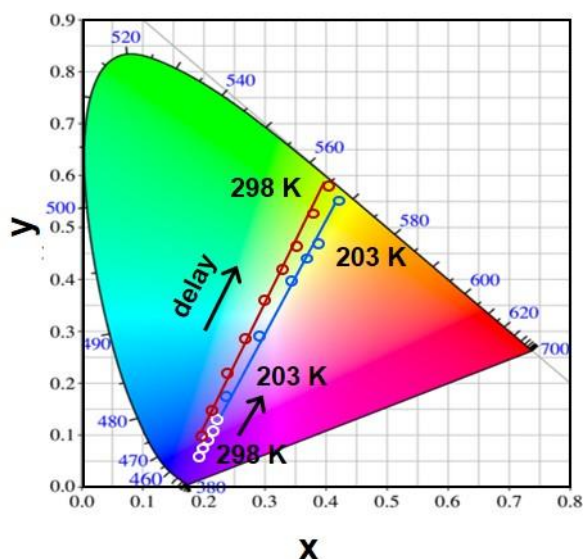


Fig. S22 (a) The Commission Internationale de l’Eclairage (CIE) coordinates of the PL spectra of the polymer films.

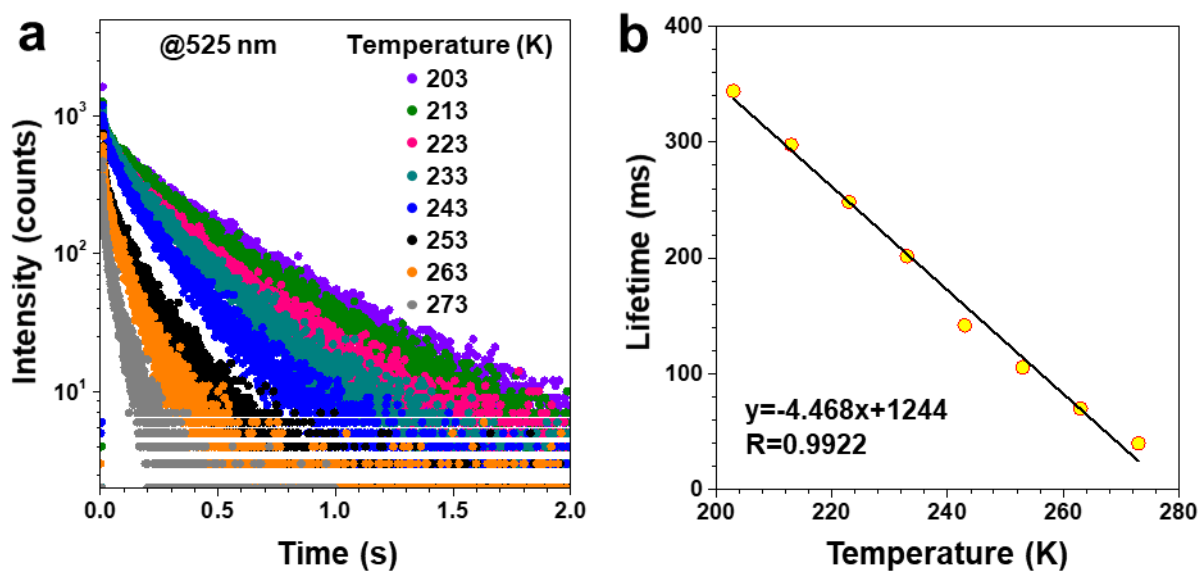


Fig. S23 (a) Lifetime decay profiles of the phosphorescence band (525 nm) at various temperatures (273, 263, 253, 243, 233, 223, 213 and 203 K, from bottom to top, respectively) and (b) the plot of lifetime against temperature for the doped polymer films.

10. Temperature sensing using PLIA based on TBBU doped polymer films

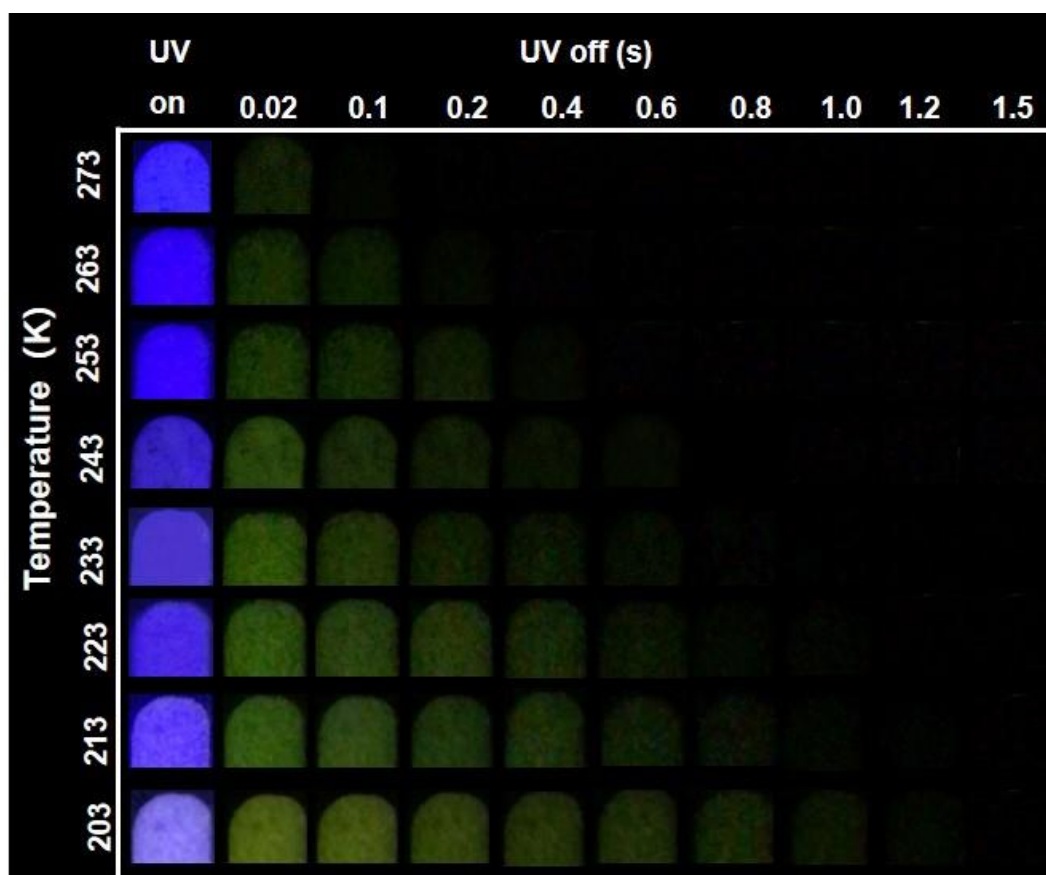


Fig. S24 Digital images of the TBBU doped polymer films at various temperatures.

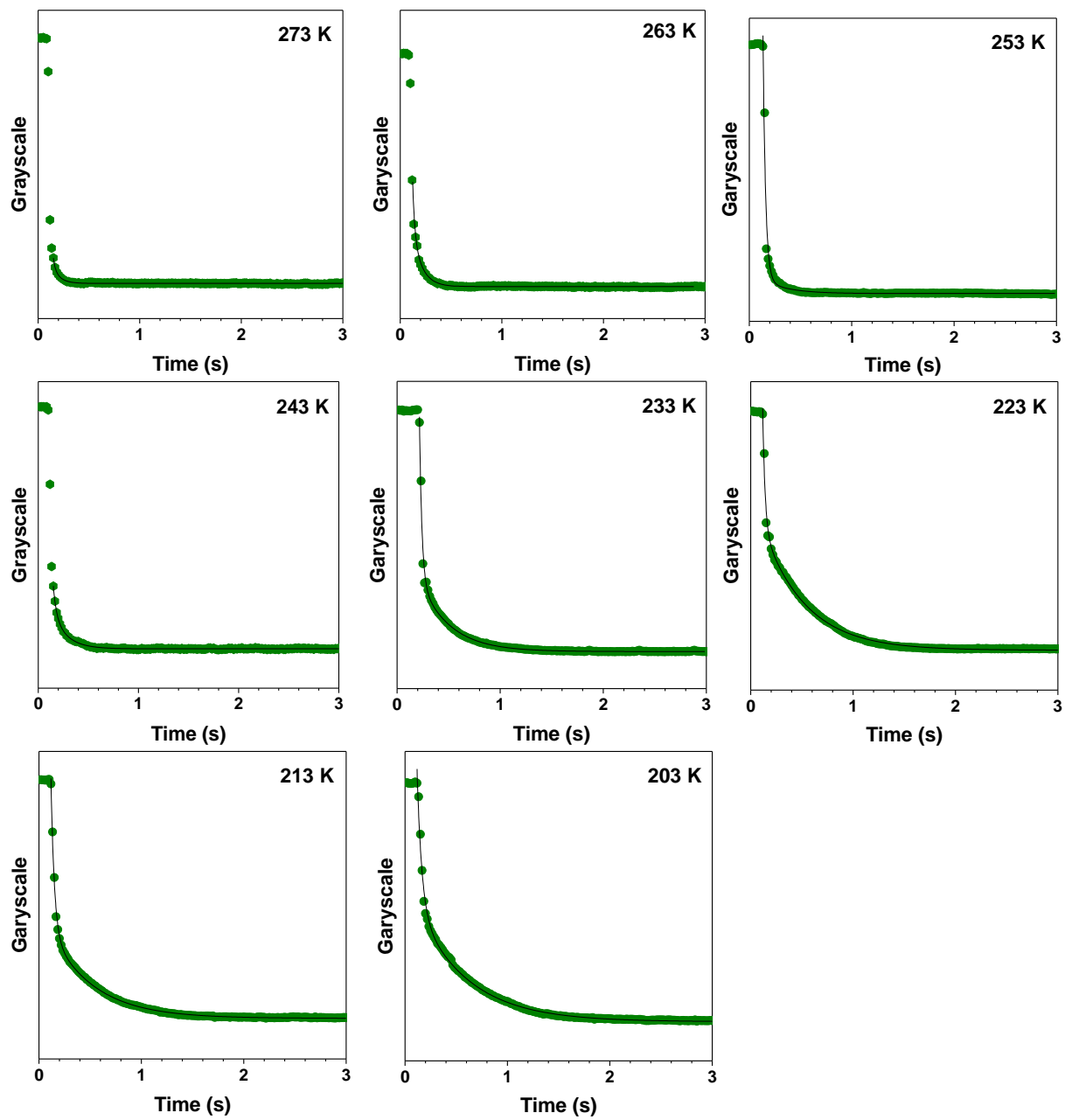


Fig. S25 The plots of G value against time for TBBU doped polymer films at various temperatures and the associated fitting curves.

Table S10 The Lifetime and calculated temperature using PLIA based on TBBU doped polymer films.

Temperature (K)	Lifetime (ms)	Average lifetime (ms)	Calculated temperature (K)	Relative error (%)
203	341, 333, 345, 336, 336	338±4.8	203±1.1	0.318
213	297, 295, 298, 298, 297	297±1.2	212±0.28	1.72
223	247, 247, 248, 246, 245	247±1.1	223±0.26	0.529
233	202, 211, 197, 204, 202	203±5.1	233±1.0	0.386
243	167, 156, 145, 166, 149	157±9.9	243±2.2	1.23
253	117, 118, 116, 119, 117	117±1.1	252±0.28	4.24
263	70.7, 67.5, 69.5, 70.8, 68.3	69.4±1.5	263±0.32	0.949
273	31.3, 27.2, 30.1, 25.1, 24.9	27.7±2.9	272±0.64	0.285

11. Testing the temperature of ice using PLIA based on the doped polymer films

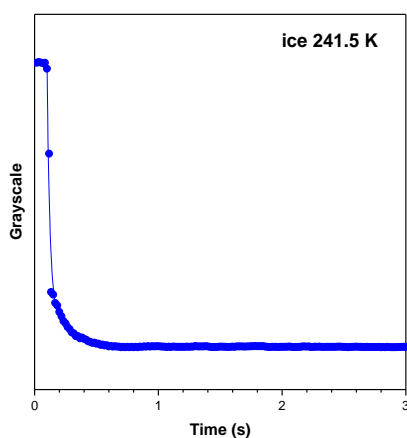


Fig. S26 Plots of G value against time of the doped polymer films on its surface.

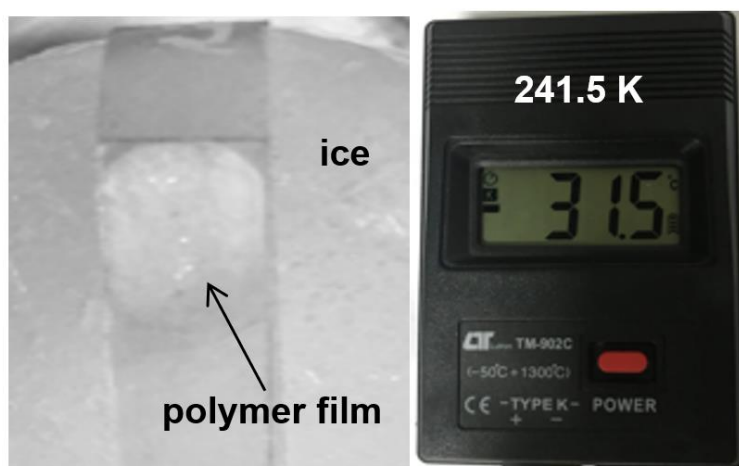


Fig. S27 Digital photos of ice with the doped films on its surface (left) and the thermometer (right).

Table S11 The lifetime and calculated temperature of ice using PLIA based on TBBU doped polymer films.

Temperature by thermometer (K)	Lifetime (ms)	Average lifetime (ms)	Calculated temperature (K)	Relative error (%)
241.5	162, 166, 167	165±2.8	241±0.42	1.19

12. Sensing temperature gradient using PLIA based on the doped polymer films

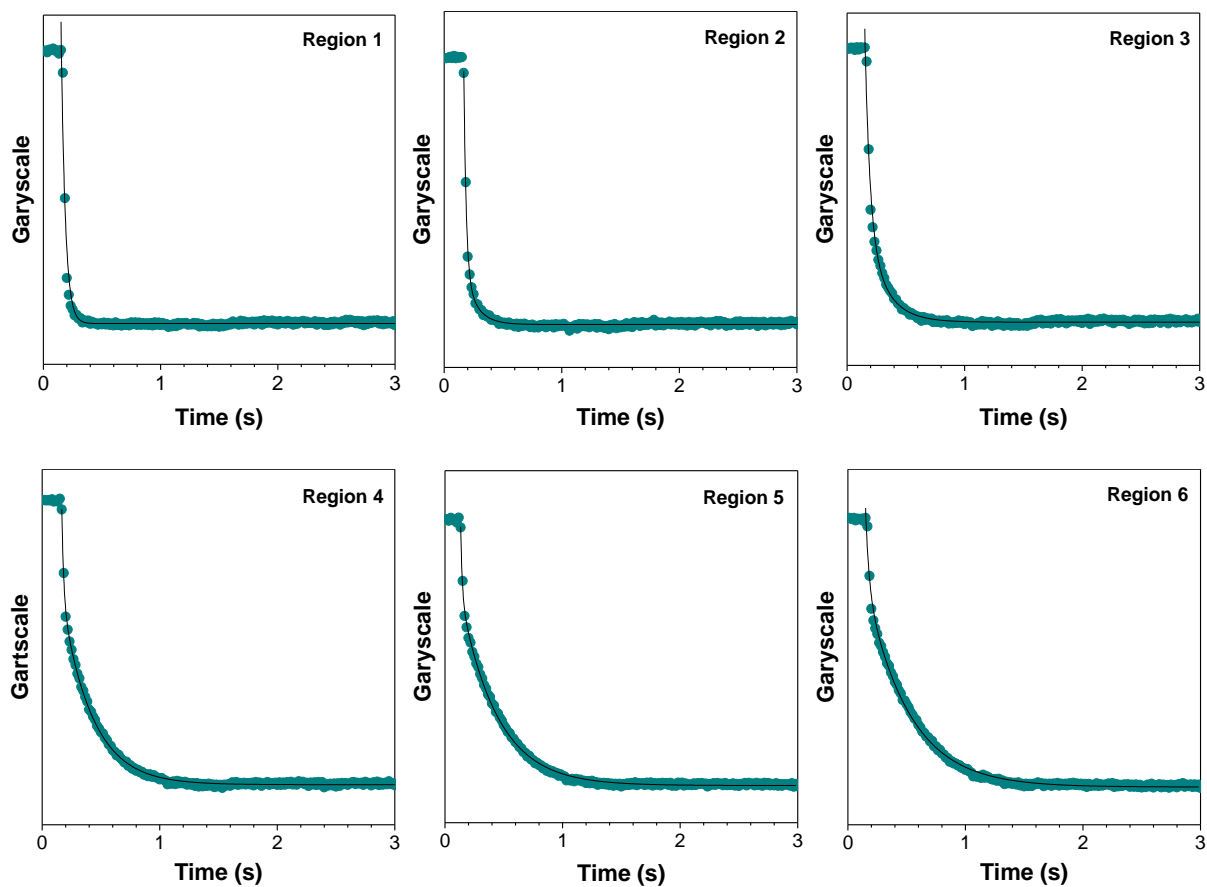


Fig. S28 Plots of G value against time of the doped polymer films at various regions of temperature gradient and the associated fitting curve.

Table S12 The lifetime and calculated temperature gradient using PLIA based on TBBU doped polymer films.

Region	Lifetime (ms)	Calculated temperature (K)
1	25	273
2	75	262
3	115	253
4	179	238
5	216	230
6	253	222

Notes and references

1. Y. Sagara, Y. C. Simon, N. Tamaoki and C. Weder, A Mechano- and Thermoresponsive Luminescent Cyclophane, *Chem. Commun.*, 2016, **52**, 5694–5697.
2. Y. Sagara, C. Weder and N. Tamaoki, Asymmetric Cyclophanes Permit Access to Supercooled Nematic Liquid Crystals with Stimulus-Responsive Luminescence, *Chem. Mater.*, 2017, **29**, 6145–6152.
3. Y. Sagara, A. Seki, Y. Kim and N. Tamaoki, Linearly Polarized Photoluminescence from an Asymmetric Cyclophane Showing Thermo- and Mechanoresponsive Luminescence, *J. Mater. Chem. C*, 2018, **10**, 8453–8459.
4. H. Zhu, S. Weng, Z. Hong, H. Yu, K. Lin, L. Z. Yu, Y. Tian and J. J. C. Yang, A Novel Carbazole Derivative Containing Fluorobenzene Unit: Aggregation-Induced Fluorescence Emission, Polymorphism, Mechanochromism and Non-Reversible Thermo-Stimulus Fluorescence, *Crystengcomm*, 2018, **20**, 2772–2779.
5. Y. Sagara, K. Kubo, T. Nakamura, N. Tamaoki and C. Weder, Temperature-Dependent Mechanochromic Behavior of Mechanoresponsive Luminescent Compounds, *Chem. Mater.*, 2017, **29**, 1273–1278.
6. S. Yamada, M. Morita, T. Agou, T. Kubota, T. Ichikawa and T. Konno, Thermoresponsive Luminescence Properties of Polyfluorinated Bistolane-Type Light-Emitting Liquid Crystals, *Org. Biomol. Chem.*, 2018, **16**, 5609–5617.
7. C. Y. K. Chan, J. W. Y. Lam, Z. Zhao, S. Chen, P. Lu, H. H. Y. Sung, H. S. Kwok, Y. Ma, I. D. Williams and B. Z. Tang, Aggregation-Induced Emission, Mechanochromism and Blue Electroluminescence of Carbazole and Triphenylamine-Substituted Ethenes, *J. Mater. Chem. C*, 2014, **2**, 4320–4327.
8. X. Luo, J. Li, C. Li, L. Heng, Y. Q. Dong, Z. Liu, Z. Bo and B. Z. Tang, Reversible Switching of the Emission of Diphenyldibenzofulvenes by Thermal and Mechanical Stimuli, *Adv. Mater.*, 2011, **23**, 3261–3265.
9. M. K. Panda, N. Ravi, P. Asha and A. P. Prakasham, High Contrast Mechanochromic and Thermo-chromic Luminescence Switching by a Deep Red Emitting Organic Crystal, *Crystengcomm*, 2018, **20**, 6046–6053.
10. T. Takeda, S. Yamamoto, M. Mitsuishi and T. J. Akutagawa, Thermoresponsive Amphiphilic

Fluorescent Organic Liquid, *J. Phys. Chem. C*, 2018, **122**, 9593–9598.

11. C. Xiaofeng, Z. Xuepeng and Z. J. C. C. Guoqing, Wide-Range Thermochromic Luminescence of Organoboronium Complexes, *Chem. Commun.*, 2014, **51**, 161–163.
12. J. Feng, L. Xiong, S. Wang, S. Li, Y. Li and G. Yang, Fluorescent Temperature Sensing Using Triarylboron Compounds and Microcapsules for Detection of a Wide Temperature Range on the Micro- and Macroscale, *Adv. Funct. Mater.*, 2013, **23**, 340–345.
13. J. Feng, K. Tian, D. Hu, S. Wang, S. Li, Y. Zeng, Y. Li and G. Yang, A Triarylboron-Based Fluorescent Thermometer: Sensitive Over a Wide Temperature Range, *Angew. Chem. Int. Ed.*, 2011, **50**, 8072–8076.
14. P. Thilagar and S. J. J. o. M. C. C. Mukherjee, Stimuli and Shape Responsive ‘Boron-Containing’ Luminescent Organic Materials, *J. Mater. Chem. C*, 2016, **4**, 2647–2662.
15. X. Liu, S. Li, J. Feng, Y. Li and G. Yang, A Triarylboron-Based Fluorescent Temperature Indicator: Sensitive Both in Solid Polymers and in Liquid Solvents, *Chem. Commun.*, 2014, **50**, 2778–2780.
16. M. Mao, R. Ming-Guang and S. J. C. A. E. J. Qin-Hua, Thermodynamics and Conformations in the Formation of Excited States and Their Interconversions for Twisted Donor-Substituted Tridurylboranes, *Chem-Eur. J.*, 2012, **18**, 15512–15522.
17. M.G. Ren, M. Mao and Q.H. Song, The Equilibria and Conversions Between Three Excited States: the LE State and Two Charge Transfer States, in Twisted Pyrene-Substituted Tridurylboranes, *Chem. Commun.*, 2012, **48**, 2970–2972.
18. Y. Cao, J. K. Nagle, M. O. Wolf and B. O. Patrick, Tunable Luminescence of Bithiophene-Based Flexible Lewis Pairs, *J. Am. Chem. Soc.*, 2015, **137**, 4888–4891.
19. Y. S. Zhou, W. Qin, C. Du, H. Y. Gao, F. M. Zhu and G. D. Liang, Long-Lived Room-Temperature Phosphorescence for Visual and Quantitative Detection of Oxygen, *Angew. Chem. Int. Ed.*, 2019, **58**, 12102–12106.